2.5 Prometheus-H Reactor Plant Overview

The Prometheus-H Power Plant is a heavy ion beam-driven commercial central station power plant. This design is also an extrapolation of today's technology advanced some 20-30 years into the future. The design emphasizes the same characteristics as the Prometheus-L Power Plant; namely, safety, environmental attractiveness, economic competitiveness, soundness of physics and engineering data, and a high degree of reliability, maintainability and availability.

The data base that supports the heavy ion power plant design builds on that for the laser system. The reactor cavity is similar to that for the Prometheus-L design. It is scaled down due to the higher cavity pressure permitted for heavy ion beam propagation through the cavity environment and to the lesser required thermal power. The higher cavity pressure is a direct outgrowth of the proposed use of self-pinching cavity transport channels, discussed in Section 4.2.3. The heavy ion driver selected by the study is a single beam LINAC coupled with intermediate, high current storage rings. This approach transfers much of the development challenge from the LINAC to the storage rings. This is attractive because it potentially leads to a cost per joule of delivered energy for the heavy ion driver that is roughly half that for the laser system as discussed in Section 4.1.2.

As noted previously, Chapter 4 discusses the rationale for choosing design options for the heavy ion power plant. Additional trade studies, design point selection basis, and detailed design definition and analyses for the reactor and balance-of-plant systems are presented in Section 6, Conceptual Design Selection and Description. This section is intended to provide the reader with a brief overview of the key features of the heavy ion beam-driven inertial fusion power plant that evolved out of the design study.

2.5.1 General Plant Features - A site plan for the Prometheus-H power plant is shown in Figure 2.5-1. The main complex is similar to that for the Prometheus-L design, but the driver building is a narrow (~10 m wide, 2.2 km long) tunnel housing the linear accelerator. The LINAC is folded at the approximate midpoint by introducing a hairpin bend. This reduces the overall size and cost of the driver facility by permitting certain support systems (e.g., cryogenic and maintenance) to be shared between accelerator legs. The accelerator is a single beam, rapidly cycled (30 kHz in a burst mode) design coupled into a stack of 14 high current storage rings that are also shown in the figure. The LINAC is actually cycled 18 times per pulse with two of the storage rings collecting three beamlets each to form a single prepulse beam for each side of the target. The beams are switched out of the storage rings into two multiple beam buncher accelerators that compress the pre and main pulses to a duration acceptable for target implosion. Upon exiting the bunchers, the group of 14 beams is divided into two sets consisting of six main and one prepulse beam and directed down

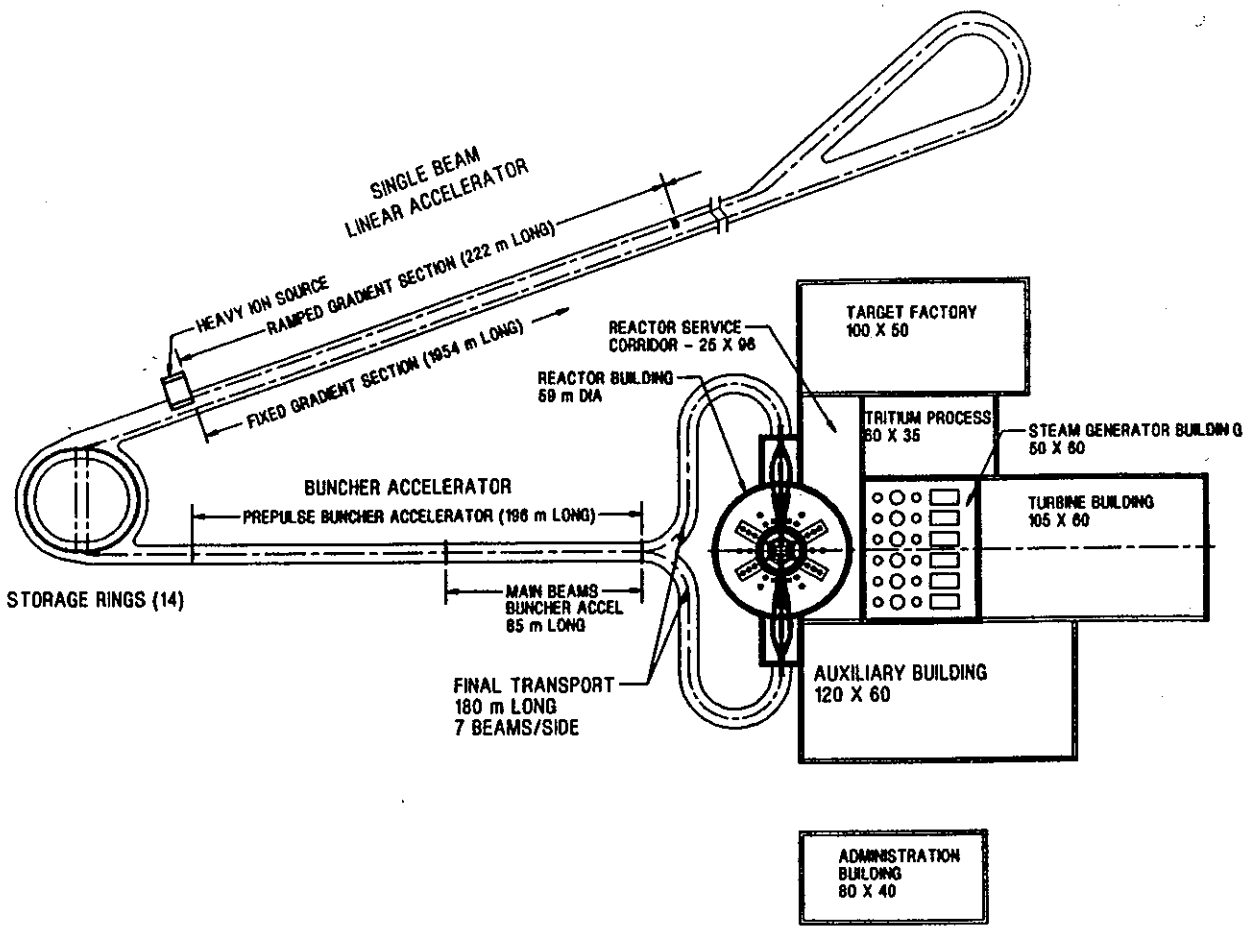

Figure 2.5-1. Heavy Ion Reactor Plant Site Plan

a final drift compression section to the Reactor Building. This is an attractive, low-cost approach to the heavy ion driver design as discussed in Section 6.

Figure 2.5-1 illustrates the other ancillary facilities necessary for the power plant. As in the laser system, the steam generator building houses six sets of steam generators for the lead and helium primary coolants. However, as indicated in Table 2.5-1, the total thermal cycle power is reduced from to 2780 MWt for this system (compared to 3264 MWt for the laser design) due to the improved heavy ion driver efficiency. This reduces the size of the main steam turbine generator from 1400 to ~1200 MWe. Sixteen percent of this gross power supports in-plant requirements for the heavy ion driver (137 MWe), auxiliary systems (28 MWe), and liquid lead pumping (25 MWe). The net power delivered to the electric grid is therefore 999 MWe.

Helium flow through the blanket is again provided by steam-driven recirculators. The tritium processing, target factory, and auxiliary buildings are comparable to their laser counterparts although their internal details are different due to the dissimilar process flows and manufacturing requirements for the heavy ion targets. It should be noted

Table 2.5-1 Prometheus-H Major Design Parameters and Features

Parameter	Value
Net Electric Power (MWe)	999
Gross Electric Power (MWe)	1189
Driver Power (MWe)	137
Auxiliary Power (MWe)	28
Cavity Pumping Power (MWe)	25
Total Thermal Cycle Power (MWt)	2780
Blanket Loop Power (MWt)	1597
Wall Protection Loop Power (MWt)	1162
Usable Driver Waste Heat (MWt)	NA
Usable Pumping Waste Heat (MWt)	21
Thermal Conversion Efficiency	42.7%
Recirculating Power Fraction	16%
Net System Efficiency	36%
Fusion Power (MW)	2543
Neutron Power (MW)	1818
Surface Heating Power (MW)	725
Fusion Thermal Power (MWt)	2797
Thermal Power to Shield (MWt)	38
Cavity Radius (m)	4.5
Cavity Height (m)	13.5
First Wall Protection/Coolant Media (In/Out Temp., °C)	Liquid Lead (375/525)
Breeder Material	Li_2O Pebbles
Structural Material, Wall and Blanket	SiC
Blanket Heat Transfer Media (In/Out Temp., °C)	1.5 MPa Helium (400/650)
Cavity Pressure (mtorr, Pb)	100
Neutron Wall Load, Peak/Ave (MW/m^2)	7.1/4.7
Energy Multiplication Factor	1.14
Tritium Breeding Ratio (TBR)	1.20
Target Illumination Scheme	Indirect Drive, Two Sided
Number of Beams	18 in LINAC (12 main + 6 in 2 prepulses)
Driver Output Energy (MJ)	7.8 (7.0 transmitted to target)
Overall Driver Efficiency (%)	20.6
Ion Accelerated	Lead
Charge State	+2
Final Energy (GeV)	4.0
Type of Accelerator	Single Beam LINAC
Final Beam Transport Efficiency (%)	90
Target Gain	103
Target Yield	719
Repetition Rate (pps)	3.5
Plant Availability (%)	80.8
Cost of Electricity (mills/kWh, 1991$)	62.6

that the target factory production capacity is only 63% of that for the laser system due to the reduced pulse repetition rate (3.54 versus 5.65 pps). The target factory cost is thus comparable to that for the laser system in spite of the fact that the heavy ion targets are more complex.

The heavy ion driver delivers 7 MJ of energy to the targets at a repetition rate of 3.54 pps. This results in a fusion yield of 719 MJ and a total power of 2792 MWt with the anticipated 1.14 energy multiplication factor. The liquid lead loop handles 1162 MWt of this power and the helium coolant loop transports 1597 MW while 38 MWt are deposited in the bulk shield as waste heat. An overall thermal cycle efficiency of 42.7% is achieved for this system as compared to 42.3% for the laser case because a larger percentage of the input heat is contained in the high temperature helium loop.

The Prometheus-H reactor cavity is essentially identical to that for the laser system. The main differences are a reduction in size from 5 to 4.5 m radius and a simplified beamline interface. These changes are a direct outgrowth of the proposed mode of cavity transport. The capability to form the proposed self-pinched heavy-ion transport channel is speculative at present, but the many engineering advantages this provides (few, small blanket penetrations, improved final focus magnet shielding, high chamber operating pressure) definitely warrant further investigation. This is highlighted by comparing Figures 2.4-7, 2.4-11, 2.5-4, and 2.5-5. The 60 individually shielded, ~1 m focal aperture laser beamlines in Figure 2.4-7 are replaced by two, 7-beam bundles of final focus magnets indicated in Figure 2.5-4. The actual focal spots are formed at the back side of the blanket and re-imaged onto the target through two 2-cm diameter openings in the blanket. This significantly reduces the amount of bulk shield material and combines with the smaller cavity size to provide a 30% reduction in reactor cavity cost for the Prometheus-H design.

2.5.2 Target Features - The TWG-referenced guidelines mentioned the use of both direct drive (DD) and indirect drive (ID) targets for the heavy ion driver but, because of the stiffness of the beams and the added complications of direct drive, the direct drive target was judged not to be worthy of further consideration. Moreover, direct drive heavy ion gain curves were never supplied.

The indirect drive target was adopted as the baseline target for the heavy ion driver. The revised target groundrules from the TWG stated that single-sided illumination of the ID target was technically possible for the target with negligible degradation of performance. For purposes of the study, it was recommended no degradation or enhancement was to be assumed for single-sided illumination. In a meeting with DOE in August 1991, members of the TWG advised the teams that the single-sided illumination option was judged to have too much technical risk to be considered as the

primary option. Thus the team elected to baseline the two-sided illumination for the ID target.

The indirect drive target employs a similar cryogenic DT capsule as the direct drive target. To provide a suitably uniform compression, a radiation case surrounds the DT capsule. The ends of the case have energy converter regions of a similar material. The heavy ion beams impinge upon the energy converter regions and convert the beam energy into X rays that bathe the inside of the case and the capsule. The radiation case will provide the radiation uniformity on the internal capsule. The capsule is suspended within the case by a very light weight support structure to withstand the injection acceleration forces yet not influence the target performance.

The Target Factory would be modified to add the step of mating the radiation case to the DT capsule and to delete the sabot process. The radiation case performs the same functions of protection as the sabot for the direct drive target.

The injection scheme for the indirect target will be based upon a pneumatic system. The support for the internal DT capsule has been determined to be able to sustain 200 g's of acceleration that establishes the length of the injector at 20 meters. A set of eight injector barrels will be used in a Gatling gun arrangement to enable the functions of loading, injecting, and evacuation be accomplished at the requisite target rate. The injector assembly will be aligned 10° off the beamline axis to provide adequate clearance with the beam final focus subsystem. Tolerances on the target final velocity will be very tight. Techniques of steering the beams will be a subject of investigation and development.

2.5.3 Heavy Ion Driver Features - The heavy ion driver must efficiently and cost-effectively deliver the required energy to the target within a focal spot radius on the order of 6-mm diameter from two sides of the cavity. The two key design choices considered for this study involved the accelerator configuration (single versus multiple beam) and the technique for delivering the beams to the target (channel transport versus some form of direct ballistic focus). The design team chose a single beam LINAC with storage rings for the accelerator configuration based on the clear economic advantage for this approach as discussed in Section 2.3. Channel transport was selected on a more qualitative basis. Channel transport offers many potential engineering advantages over focusing the beams directly on the target. Furthermore, analyses indicate that, when the beams are partially stripped, there is more than enough beam current to support the formation of a self-pinching transport channel. The concern lies in the capability to maintain a stable 5.6 m long channel in the surrounding cavity environment and the repeatability of aiming this channel at the proper spot on the target. These are critical issues that can only be addressed through future theoretical and experimental work. Section 4.3 discusses the detailed rationale

for selecting these technology options for the heavy ion driver. The remainder of this section presents a summary of the final heavy ion driver design.

The systems studies led to the selection of a 7 MJ target incident energy design point for the Prometheus-H design point. A 10% energy loss was budgeted for forming the beam transport channels and transmission to the target, so the LINAC is designed to output 7.8 MJ. Lead ions with a +2 charge state were chosen for compatibility with the first wall protection scheme. Detailed studies of transport lattice scaling determined that the required 7.8 MJ could be provided with 4 GeV ions using only 18 beamlets. Low ion energies are desirable because they provide improved target performance; however, the number of beamlets is a concern at low energies because it can become quite large (>50) for some lattice scaling choices. This is a particular problem for the single beam LINAC because of core recycling losses and beam stability and scattering loss in the high current storage rings. Section 6.2 discusses the trade studies that led to the 18 beamlet design point.

The resulting beamline configuration at various points along the driver is illustrated in Figure 2.5-2. Corresponding beam and LINAC parameters are summarized in Table 2.5-2. The driver consists of an injector, a ramped gradient section, a fixed gradient section, a stack of storage rings, a buncher accelerator section, a drift compression section, and a final focus section. These are shown in plan view in Figure 2.5-1. Switching sections will also be required to insert and extract the beams from the storage rings, but these were not specifically considered for this study.

The overall length of the LINAC is 2.2 km. Transport lattice scaling was chosen so the mean beam radius of 9.4 cm remains constant over this entire distance. Additional constraints were imposed on quadrupole axial packing fraction (< 80%) and aspect ratio (beam radius/quadrupole length < 0.25). These lead to a common magnet radial build as indicated in Figure 2.5-2; however, the magnet length and field strength must be adjusted to provide proper focusing. The quadrupole inner and outer radii were chosen as 1.65 and 3.3 times the mean beam radius based on guidance provided by LBL. An additional 12 cm was added to the magnet outer radius to determine the core inner radius. This provides space for cryogenic insulation, magnet dewar, insulator rings, accelerator structure, and vacuum access.

Ions are injected into the LINAC at an energy of 6 MeV. The beamlet current is 14 A at this point and the pulse length is 15.5 μs. The initial voltage gradient is low (~40 kV/m), but it rapidly increases to the design limit of 1 MV/m over the 223 m ramped gradient section. The local voltage gradient scales with beam energy in this section is based on accepted limits as discussed in Section 6.2. This section contains 300 quadrupoles, terminating at a beam energy of ~100 MeV where the limiting gradient is reached. The initial 70% quadrupole axial packing fraction is high (but less

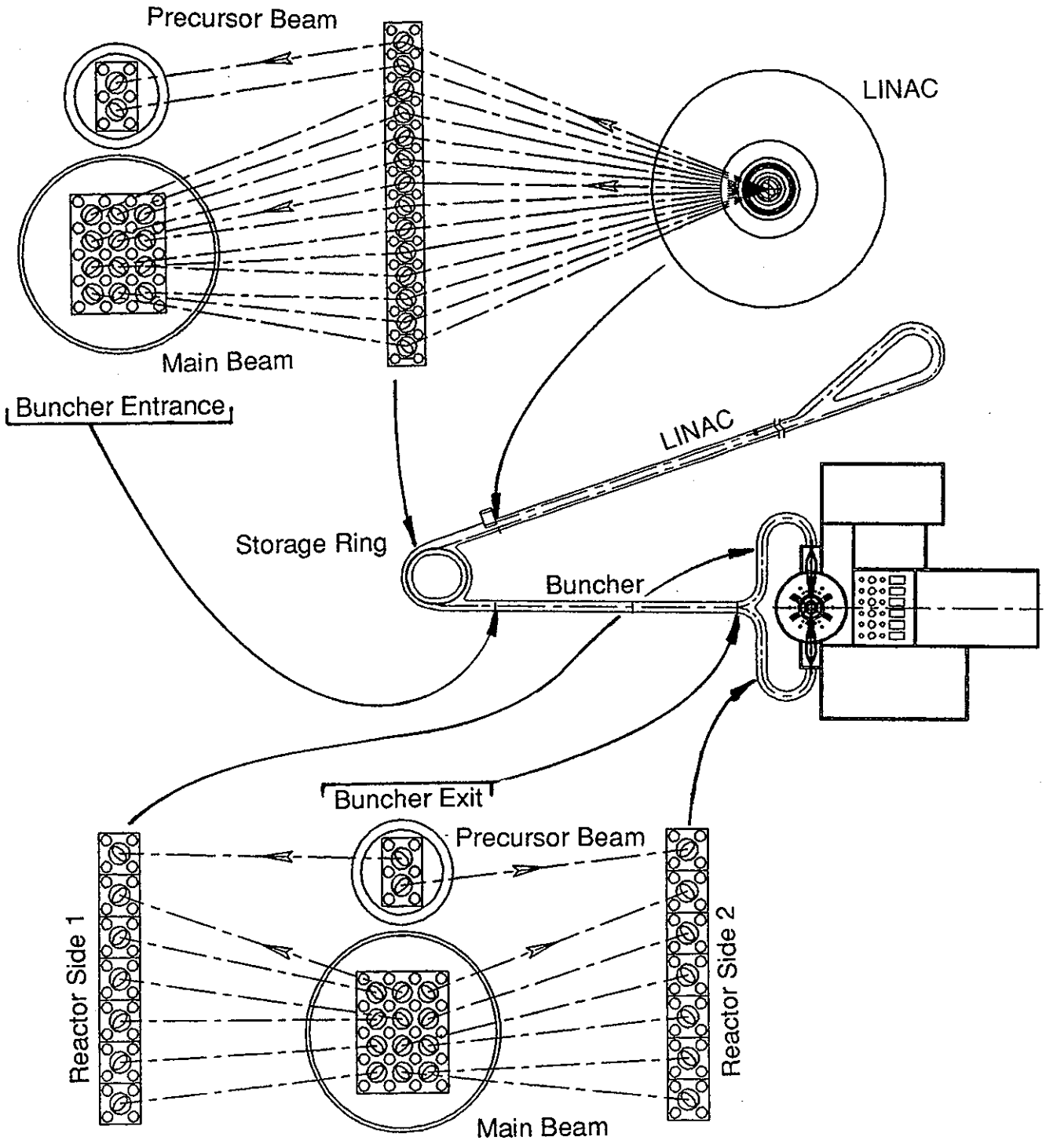

Figure 2.5-2. Beamline Configuration – Routing from LINAC to Reactor

Table 2.5-2. Parameter Summary for Prometheus-H Driver Design

Parameter, Unit	Injector	Trans	Final	Main Beamlets		Prepulse Beamlets	
				Buncher	Fnl Focus	Buncher	Fnl Focus
Beam Energy, MeV	6	99.4	4000	4000	4000	4000	4000
Beam Radius, cm	9.4	9.4	9.4	9.9	15.0	10.5	14.9
Lattice Half Period, m	0.50	1.33	4.85	4.67	3.55	4.50	3.56
Pulse Length, ns	15,500	1639	85.3	70.5	17.8	176.4	54.4
Bunch Length, m	36.5	15.7	5.1	4.2	1.07	10.6	3.27
Beamlet Current, A	14	132	2532	3065	12,130	3674	11,920
Packing Fraction, %	69.0	39.3	18.8	21.5	56.2	24.4	55.5
Magnet Length, m	0.344	0.523	0.911	1.00	1.99	1.10	1.98
Magnet Bore Radius, m	15.5	15.5	15.5	16.4	24.8	17.3	24.7
Magnet a/L Ratio	0.273	0.179	0.103	0.099	0.075	0.096	0.076
Core Inner Radius, cm	43.0	43.0	43.0	155.4	—	68.0	—
Core Thickness, cm	36.9	150.2	7.8	6.5	0.0	16.2	0.0
Depressed Tune, Deg	8	5.3	3.0	2.6	0.86	2.2	0.87

Parameter, Unit	Ramped Gradient	Fixed Gradient	Storage Ring	Main Buncher	Main Drift	Prepulse Buncher	Prepulse Drift
Number Beams	1	1	14	6	6	1	1
Section Length, m	223	1954	157	85	180	196	180
Tunnel Width, m	9.8	9.7	8.1	8.1	8.1	8.1	8.1
Core Volume, m^3	906	1629	—	60	—	193	—
Pulser Energy, MJ	0.13	1.9	0	0.49	0	0.59	0
Number Quadrupoles	300	578	34	18	39	41	37
Number Dipoles	—	—	32	—	19	—	20
Dipole Lengths, m	—	—	2.40	—	2.30	—	2.15
Magnet Powers, MW	0.9	1.734	0.198	0.054	0.348	0.123	0.342

than the 80% design limit) because focusing is needed every 0.5 m at this energy (lattice half period). The packing fraction decreases to 39% at the end of the ramped gradient section because the lattice half period grows to 1.33 meters.

The fixed gradient section (1 MV/m) continues from the 100 MeV point to the final energy of 4 GeV. This section is 1.95 km long and contains 578 quadrupoles. The pulse length decreases from 1.64 μs to 85 ns in this section, so the beamlet current increases from 132 A to 2.53 kiloamps. The quadrupole packing fraction drops to 19% at the end of the fixed gradient section because the lattice half period has grown to 4.85 meters. The quadrupole length also increases, from 0.52 to 0.91 meters, to offset the increased beam stiffness.

A flux swing of 1.5 T was selected to reduce induction core losses (proportional to ΔB) since they are recycled 18 times per pulse for this design. The corresponding core thickness increases from 37 to 107 cm in the ramped gradient section due to the increase in gradient. Thereafter, it decreases because the pulse length shortens as the beam energy increases. Driver efficiency was a concern for the single beam design, but the 1.5 T flux swing and low number of beamlets lead to a projected efficiency of 20.6% for the Prometheus-L driver using Metglas loss curves suggested by LBL. This is discussed in more detail in Section 4.1.

The target pulse is generated by operating the LINAC in a burst mode. The 18 beamlets are sequentially accelerated by cycling the induction cores on a 30 kHz timescale so the longest residence time within the storage rings is less than 1 ms. The beamlets are stacked vertically in 14 storage rings as indicated to provide a common bend radius and path length. Only 14 storage rings are needed because two storage rings collect three beamlets each to form a single prepulse for each side of the target. The twelve remaining rings each collect single beamlets that are used to form the main target pulse. This arrangement provides the recommended prepulse energy content of ~30%.

Once all beamlets are collected and properly time sequenced, they are released from the storage rings and sent to the two buncher accelerators as indicated in Figure 2.5-2. The prepulse buncher is 196 m long and induces a 4.9% velocity tilt on these beamlets. This causes the 256 ns long prepulse to compress to the required 30 ns over the 180 m drift distance to the target. The main pulse beamlets are sent through a shorter 85 m long buncher since they only require a 2.1% velocity tilt. This compresses their pulse length from 85 ns to the 7.3 ns required for target implosion over the same 180 m drift distance. The final time phasing and energy content of the prepulse and main beamlets is shown schematically in Figure 2.5-3. A multiple-beam transport lattice is employed in the buncher sections, as indicated, to minimize core volume.

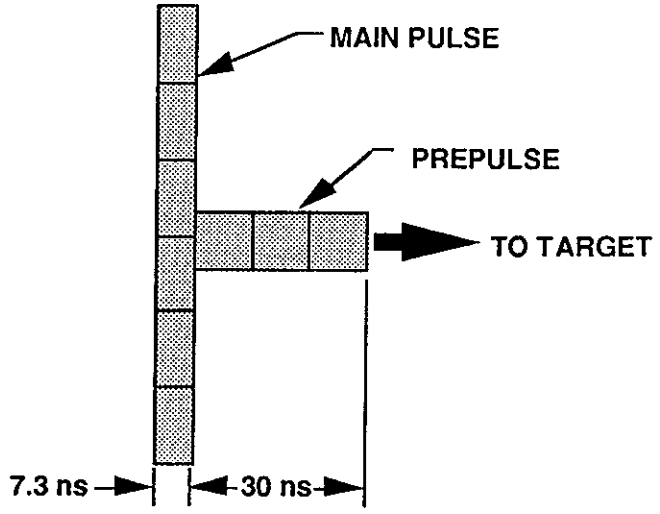

Figure 2.5-3. Heavy Ion Beam Prepulse and Main Pulse Schematic

After the beams exit the buncher section they are divided as indicated in Figure 2.5-2 with six main and one prepulse beamlet directed to each side of the reactor cavity. The beam radius is allowed to increase in the buncher and drift sections to ease matching with the final focus magnets. The physical arrangement of the final focus magnets and beamlines is illustrated in Figure 2.5-4. Triplet quadrupoles are used to focus the beams down on a point at the rear surface of the blanket. A lead vapor cell provides electrons that space-charge neutralize the beam at the exit of the last quadrupole. This permits the final 6-mm diameter focal spot to be attained.

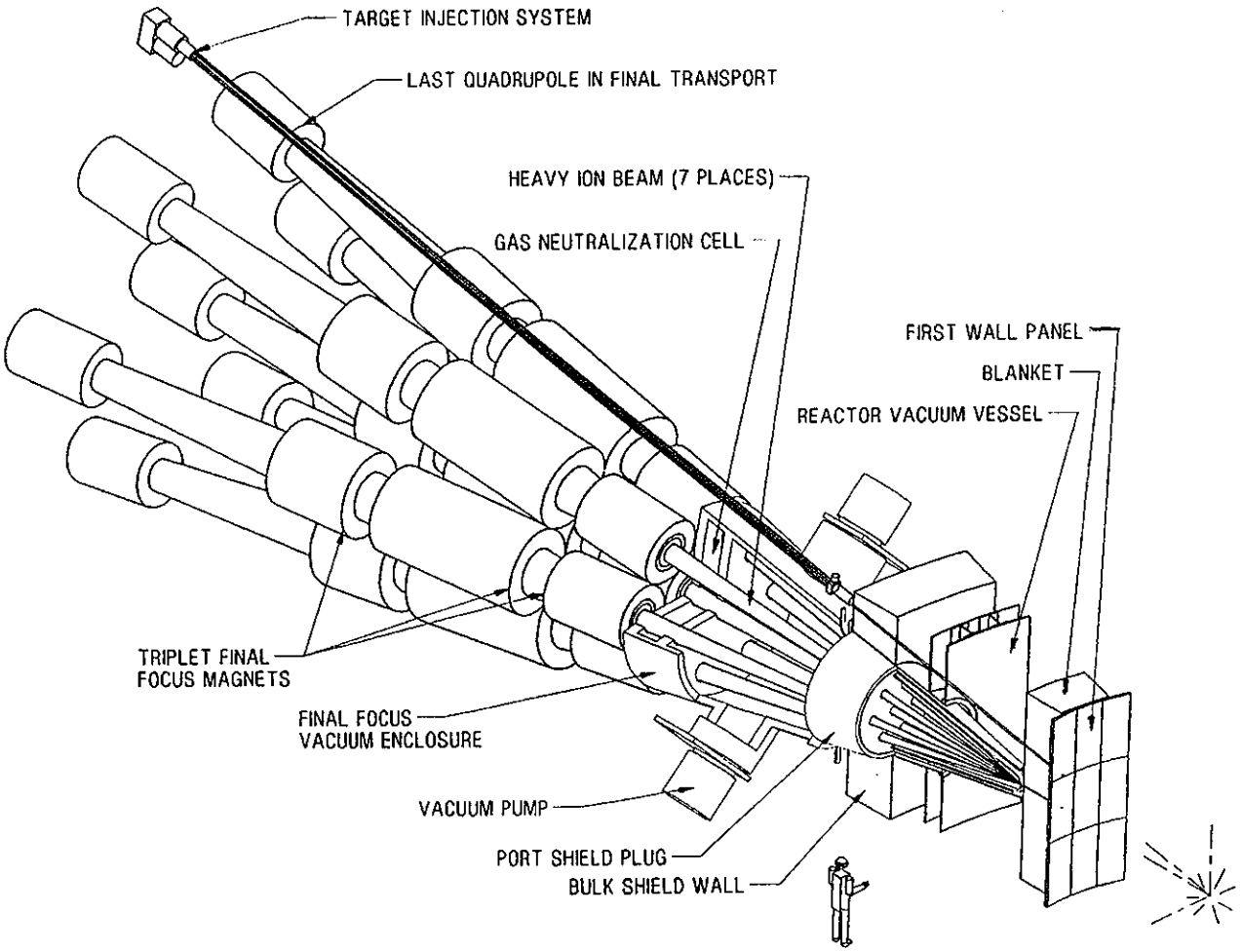

Figure 2.5-4. Physical Arrangement of Final Focus Coils, Plenum, and Shielding Penetrations

At the focal point, a lead vapor jet is provided that strips the beam ions to a high charge state. This is the mechanism for creating the transport channel. It also serves to isolate the reactor cavity pressure environment (~100 mtorr) from that required in the beamlines (~0.01 mtorr). The prepulse beamlet is located on the channel axis and arrives first at the lead gas jet as indicated in Figure 2.5-4. The six main beamlets follow immediately and they arrive in parallel. Both the prepulse and the main pulse have a significant current margin for self-pinching (greater than five times), so channel

formation is certainly feasible. The surrounding plasma's tendency to generate a reverse current that might destroy the channel is a concern. This is identified as a critical research and development issue in Section 5.

If transport channels are found to be viable, questions still remain concerning the ability to direct them at a target that is 5.6 m away with an accuracy of ±1 mm. The initial path of the pinched beam channel will be defined by its net momentum. The single prepulse beams can be steered directly and can easily be pointed with the required accuracy. The direction of the main pulse, however, depends on the momentum balance between the six main beamlets. The questions involve whether momentum imbalances cause steering of the channel or if the prepulse beam provides a focusing mechanism. These questions are a related part of the transport channel critical issue.

2.5.4 Reactor Cavity Features - Figure 2.5-5 depicts the final Prometheus-H reactor cavity configuration. The design is essentially the same as that for the laser system. The most notable difference is the simplified beamline interface. The laser driver requires 60 beam penetrations through the blanket that vary in diameter from 17 to 26 cm and force the outer wall of the building to be located at a diameter of

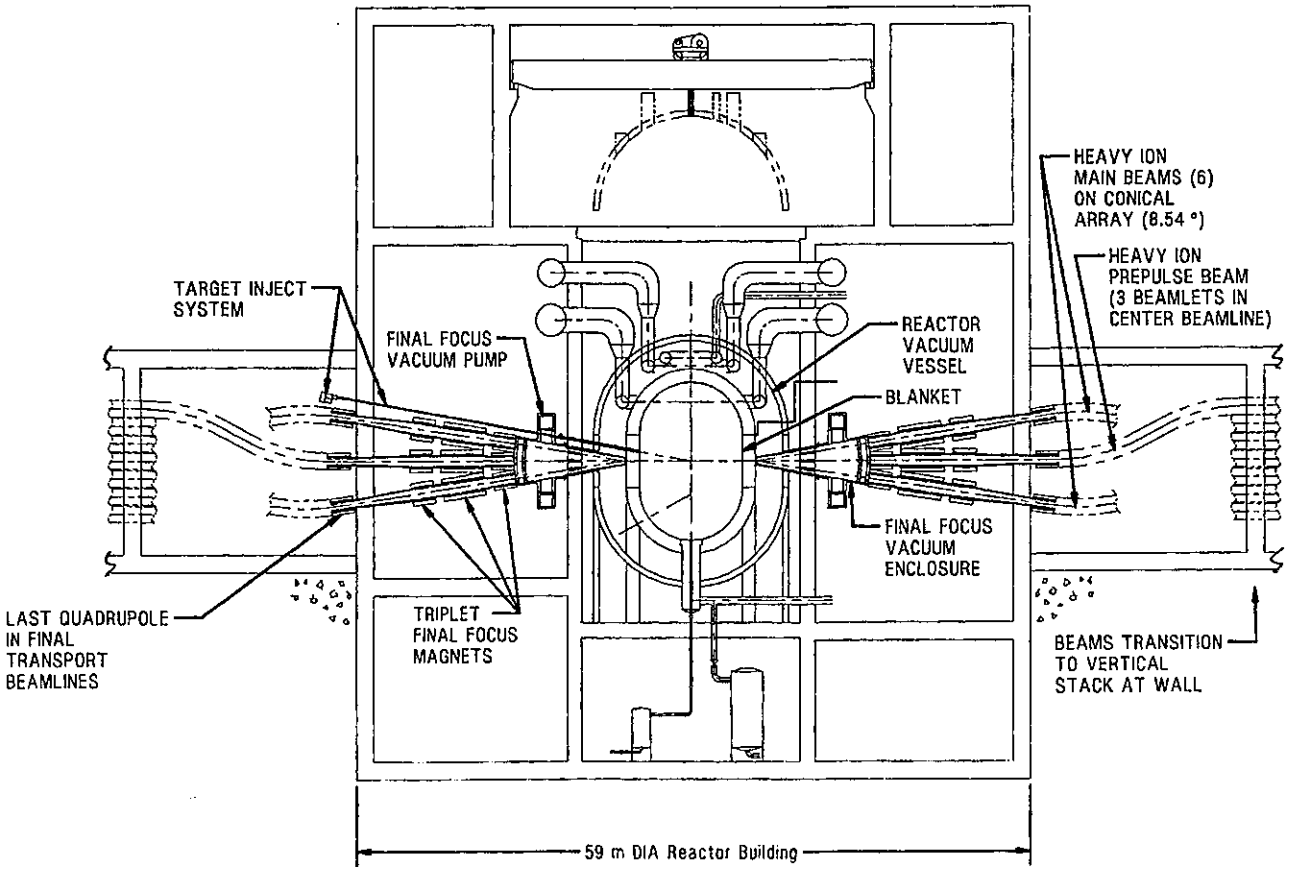

Figure 2.5-5. Prometheus-H Reactor Cavity Arrangement

86 meters to provide adequate separation distance for protecting the final optics from radiation damage. These are replaced by two, 2-cm diameter openings for the heavy ion driver as indicated in Figure 2.5-4. The localized nature of the heavy-ion beamlines permits shielding them using two adjoining enclosures as indicated in Figure 2.5-1. The overall building diameter is thus reduced to 63 meters.

The other configuration difference is the 0.5 m reduction in cavity radius. A smaller size cavity is possible based on cavity clearing calculations, but significant modifications in the wall and blanket design would be required to accommodate the increased wall loading and power density in the blanket. Reductions in component reliability and lifetime would also be expected under these conditions. For the 4.5 m final design point, the lifetime of the first wall and blanket remain roughly the same as predicted for the laser first wall and blanket. Furthermore, all structural, thermodynamic, safety, and environmental impact analyses conducted for the laser cavity are directly applicable to the heavy ion design. Some safety margins are reduced, but the conclusions are still valid.

The 4.5 m radius Prometheus-H cavity design thus achieves many of the cost benefits of smaller size without compromising the attractive design features. The building diameter is reduced from 86 to 63 meters because the need to protect final line-of-sight optics is eliminated. The final focus magnet arrangement allows close placement of ancillary equipment and service buildings and localized beamline shielding. The energy conversion system is based on the same general features and hardware as the laser plant. Piping sizes are identical to those for their laser counterparts. The only real difference is the elimination of a driver waste heat recovery system since this is not practical for the heavy ion driver.

Vacuum pumping requirements for the heavy ion system are less severe due to the increased cavity pressure. The vacuum ports are identical to the laser reactor chamber, but simple roots blowers were found to provide adequate pumping speed and capacity. There is a common vacuum chamber housing all the beamlines from the last quadrupole in the triplet set to the focal point. Pressure in this region is maintained by two cryogenic vacuum pumps due to the 0.01 mtorr requirement during final focus. Shielding around this enclosure is equivalent to that provided around the laser beamlines. Shielding is also provided on the blanket facing surface of the last focusing magnet and within the bores of these magnets, but thicknesses are minimal because the magnets are not exposed to primary radiation. This permits all focusing magnets to be superconducting with the possible exception of the central, prepulse triplet that does have direct line-of-sight into the cavity.

The majority of the driver building is a simple tunnel housing the single beam LINAC. The tunnel is enlarged for the storage ring, buncher accelerator and drift compression sections to accommodate the multiple transport channels in these sections. Considerable care was taken in arranging these sections to preserve the proper drift

lengths, beam bend radii, and quadrupole placements. Beamline layouts were chosen to facilitate the use of common magnet cryostats where identical parallel transport channels are required.

2.5.5 Summary of Prometheus-H Power Plant Key Features - The Prometheus-H power plant represents a very attractive design goal for heavy ion inertial fusion energy. The design embodies several potential ways to help reduce the cost and improve the engineering feasibility of heavy ion drivers. The driver plant equipment is estimated to cost $403M in 1991 dollars for a tenth-of-a-kind plant. This is significantly lower than that previously envisioned for induction LINAC drivers[2] and, in fact, corresponds to roughly half the cost per joule projected for the Prometheus-L driver.

In addition, the high efficiency of the heavy ion driver allows a reduction in the size of most of the remaining balance-of-plant systems, which translates into lower capital costs. As a result, the total direct capital cost for the Prometheus-H power plant is $1.94B; that is $230M lower than that for the laser system. Adding indirect costs increases these values to $3.63B and $430M, respectively. The projected cost of electricity for the heavy ion plant is therefore 62.6 mills/kWh; that is 13% below that for the Prometheus-L design. This is very competitive with costs projected for other advanced energy sources.

Many of the reactor and BOP features are common between the heavy ion and laser plants, but there are some distinct advantages that favor the heavy ion system. The self-formed transport channel concept significantly eases the job of designing a remote maintenance system for the first wall and blanket. It also improves the overall reactor engineering feasibility by providing a nearly uniform first wall and blanket. It mitigates concerns about the protective lead film integrity around openings, concerns about the design of effective shielding around multiple beamlines, and concerns about shielding the final focus magnets from the cavity radiation environment. Consequently, it enhances the level of safety assurance for the entire plant, although both the laser and heavy ion designs are anticipated to achieve the highest LSA rating of one. Finally the reliability and maintainability assessment indicates that the heavy ion plant will have an 80.8% plant availability; that is 1.4% higher than that predicted for the laser plant.

References for 2.5

1. J. P. Holdren, Chair, et. al., "Report of the Senior Committee on Environmental, Safety, and Economic Aspects of Magnetic Fusion Energy," UCRL-53766, 25 September 1989.

2. D. S. Zuckerman, et al., "Induction LINAC Driven Heavy Ion Fusion System Model," Fusion Technology, Vol 13, #2, 1986.